nature geoscience

SUPPLEMENTARY INFORMATION

DOI: 10.1038/NGEO662

Emergence of sprite streamers from screening-ionization waves in the lower ionosphere

Alejandro Luque*, Ute Ebert[1,2]

[1] *Centrum voor Wiskunde en Informatica (CWI), P.O. Box 94079, 1090 GB Amsterdam, The Netherlands, email: luque@cwi.nl, ebert@cwi.nl, +31-20-592 4206 (tel Ebert), 4199 (fax) and*

[2] *Dept. Appl. Physics, Eindhoven Univ. Techn., The Netherlands*

(Dated: July 23, 2009)

We use the discharge model described in [19] and extend it by electron attachment to oxygen and by altitude-dependent transport and ionization parameters:

$$\begin{aligned}
\partial_t n_e &= \nabla \cdot (n_e \mu(N)\mathbf{E}) + \nabla \cdot (D(N)\nabla n_e) \\
&\quad +(\nu_i - \nu_{att})n_e + S_{ph}, && (1)\\
\partial_t n_+ &= \nu_i n_e + S_{ph}, && (2)\\
\partial_t n_- &= \nu_{att} n_e, && (3)\\
\nu_i &= \mu(N)|\mathbf{E}|\alpha_i(N)e^{-E_i(N)/|\mathbf{E}|}, && (4)\\
\nu_{att} &= \mu(N)|\mathbf{E}|\alpha_{att}(N)e^{-E_{att}(N)/|\mathbf{E}|}, && (5)\\
\epsilon_0 \nabla \cdot \mathbf{E} &= \mathrm{e}(n_+ - n_-), \quad \mathbf{E} = -\nabla\phi. && (6)
\end{aligned}$$

Here N is the altitude dependent number density of neutral air molecules, $\mu(N)$ is the electron mobility, $D(N)$ is the electron diffusion, $\alpha_i(N)$ and $\alpha_{att}(N)$ are the inverse of the mean free paths of electrons between ionization or attachment events, respectively, and e is the elementary charge. Ion mobility, much smaller than electron mobility, is neglected. The term S_{ph} stands for the non-local photo-ionization according to the standard model for oxygen-nitrogen mixtures [23]. In its standard formulation that model assumes a homogeneous density of absorbing O_2 molecules and hence an isotropic absorption function. This assumption does not hold for sprites. However, we use the following approximation:

$$S_{ph}(\mathbf{r}) = \frac{\xi A(N(Z))}{4\pi} \int \frac{h(N(Z)|\mathbf{r} - \mathbf{r}'|)S_i(\mathbf{r}')d^3(p\mathbf{r}')}{|N(Z)\mathbf{r} - N(Z)\mathbf{r}'|^2},$$

where $S_i = \nu_i n_e$, $A(N)$ is a quenching factor, h is the (isotropic) absorption function of ionizing radiation [23] and Z is the z-coordinate of the maximum of $\nu_i n_e$. Here we are assuming that photo-ionization is relevant only close to the tip of a propagating front, where the impact ionization is highest. This approximation is justified by the result presented in the main text of the article: during a first stage of propagation, photo-ionization plays a minor and mostly local role. Later it becomes important for the propagation of thin streamers but their diameter as well as the photo-ionization length are then much smaller than the decay length of $N(z)$.

The number density at a given altitude z is taken as $N = N_0 \exp(-z/h)$, where $h = 7.2\,\mathrm{km}$ and $N_0 = 2.5 \cdot 10^{19}\,\mathrm{cm}^{-3}$ is the air density at ground level. The dependence of equations (1)-(5) on the neutral density is detailed in [19]; it is $\mu(N) = N_0\mu_0/N$, $D(N) = N_0 D_0/N$, $\alpha_i(N) = N\alpha_{i0}/N_0$,

DOI: 10.1038/NGEO662

Parameter	Value at ground level	Scaling factor
Electron mobility	$\mu_0 = 380\,\mathrm{cm^2\ V^{-1}\ s^{-1}}$	N_0/N
Electron diffusion rate	$D_0 = 1800\,\mathrm{cm^2 s^{-1}}$	N_0/N
Townsend ionization rate	$\alpha_{i0} = 4332\,\mathrm{cm^{-1}}$	N/N_0
Townsend ionization field	$E_{i0} = 2 \cdot 10^5\,\mathrm{V\ cm^{-1}}$	N/N_0
Townsend attachment rate	$\alpha_{att0} = 20\,\mathrm{cm^{-1}}$	N/N_0
Townsend attachment field	$E_{att0} = 3 \cdot 10^4\,\mathrm{V\ cm^{-1}}$	N/N_0

TABLE I: Parameters of our model, with their values at ground level and how they scale with the air molecule number density N. Here N_0 is the air molecule number density at ground level.

$\alpha_{att}(N) = N\alpha_{att\,0}/N_0$, $E_i(N) = NE_{i0}/N_0$, $E_{att}(N) = N\alpha_{att\,0}/N_0$, $A(N) = N_q/(N + N_q)$ with $N_q \approx 0.08N_0$ [12] where X_0 indicates the value of X at sea level, taken as in [19]. A summary of the model parameters and their values at ground level is provided in Table I.

The dependence on the air density of the impact ionization and attachment rates becomes clearer by noticing that $\mu(N)\alpha_{i,att}(N) = \mu_0\alpha_{(i,att)0}$ does not depend on N. Therefore one can write $\nu_{i,att} = Nf_{i,att}(|E|/N)$; this means that the number of impact ionization or attachment events produced by a given electron density at a given reduced electric field is proportional to the number density of air molecules.

We assume that initially the atmosphere is electrically neutral but with a pre-ionization $n_e(z) = n_+(z) = n_{e\,0}\exp(z/\ell)$ where $\ell = 2.86\,\mathrm{km}$ and $n_{e\,0} = 7.6 \cdot 10^{-14}\,\mathrm{cm^{-3}}$ [30]. This profile is based on night-time observation in conditions of normal weather. Figure 4 shows a comparison of this profile with others in the literature. Note that due to radioactivity, the actual ionization at ground level is much higher that $n_{e\,0}$ and our expression is only valid at mesospheric altitudes.

The charged thunderstorm cloud that induces the sprite discharge is simulated by a point charge located at $L_Q = 10\,\mathrm{km}$ above ground that increases linearly in time due to a constant cloud-earth current of $J = 30\,\mathrm{kA}$. The current moment change is hence $JL_Q = 300\,\mathrm{kA\,km}$ and the charge moment change at time t is $CMC = JL_Qt$. This is a simplified model of the current moment waveform for a short-delayed sprite reported in [24].

To solve the equations numerically we assume cylindrical symmetry around the vertical axis through the cloud charge; and we solve the Poisson equation between ground level and 85 km, assuming that the earth is a perfect conductor and that above 85 km the time response of the

DOI: 10.1038/NGEO662
nature geoscience

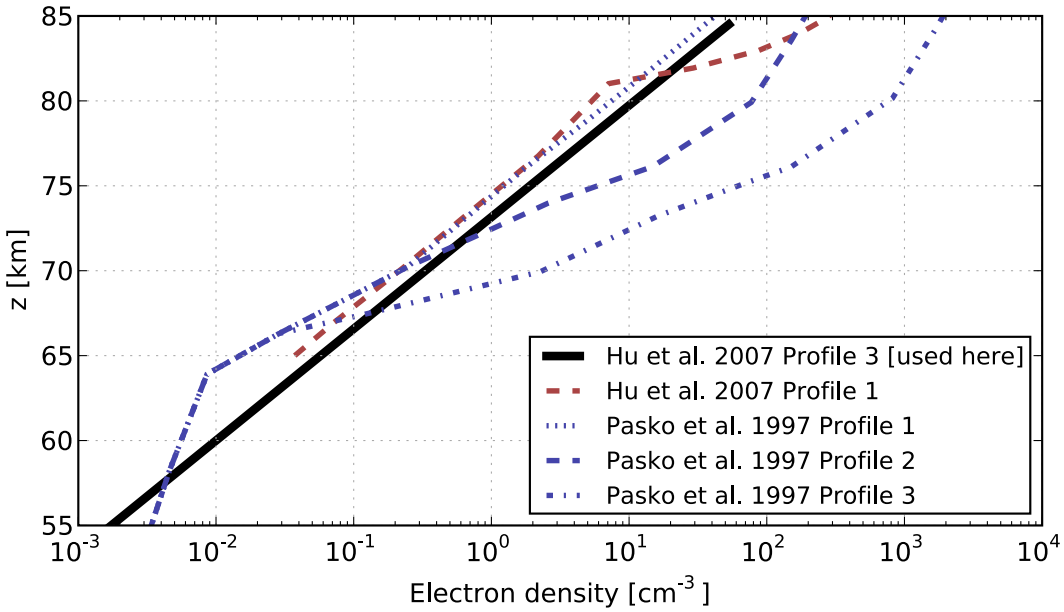

FIG. 4: Initial electron density used in our simulation (solid, thick line) and some other profiles found in the literature. Hu et al. refers to [25]; Pasko et al. refers to [17].

ionosphere, shorter than 0.2 ms is fast enough compared to our typical times to replace it by a perfect conductor as well. To make computations faster, we restrict the solution of the density equations to a layer between 55 km and 85 km. Both for the densities and for the Poisson equation, the domain extends up to a radius of 20 km in the lateral direction, where homogeneous Neumann boundary conditions (that create symmetry planes) are imposed for the particle densities.

The electric field is calculated in two parts: the cloud charge is represented by a point charge and conducting earth and ionosphere above 85 km altitude are represented by a sequence of 2 mirror charges on each side. Then we add the fields created by the charges of sprite halo and sprite streamer, obtained by solving the Poisson equation inside a cylinder that extends from ground level to 85 km and has a radius of 20 km, using homogeneous Neumann boundary conditions in the lateral boundaries and homogeneous Dirichlet in the upper and lower boundaries.

We solve equations (1)-(6) in adaptively refined grids as described in [13,23] with a maximum grid size of $\Delta r_{max} = \Delta z_{max} = 100$ m and a minimum of $\Delta r_{min} = \Delta z_{min} = \Delta z_{max}/32 \approx 3$ m. We also tested our simulations on minimal grids of 4 and 2 m. This did not change significantly the time of streamer emergence and the velocity and diameter of the sprites. Given also the relevant length scales discussed in the text and visible in the figures, we conclude that the numerical grid is fine

DOI: 10.1038/NGEO662

enough to appropriately resolve the structures.

Comparison with weakly non-linear models

The model (1)–(6) can also be written in terms of the charge density $\rho = \mathrm{e}(n_+ - n_- - n_e)$, the atmospheric conductivity $\sigma = \mathrm{e}\mu n_e$ and the ionic charge balance $\rho_i = \mathrm{e}(n_+ - n_-)$, where we have dropped the dependence on the neutral gas density to simplify the notation. From (1)-(3) we trivially obtain a charge conservation equation

$$\partial_t \rho = -\nabla \cdot \mathbf{j} \tag{7}$$

where $\mathbf{j} = \sigma \mathbf{E} + \mathrm{e}D\nabla n_e$ is the electrical current. Subtracting (3) from (2) we also obtain

$$\partial_t \rho_i = (\nu_i - \nu_a)\sigma/\mu + \mathrm{e}S_{ph}. \tag{8}$$

And if we multiply (1) with $\mathrm{e}\mu$ we get

$$\partial_t \sigma = \mu \nabla \cdot \mathbf{j} + (\nu_i - \nu_a)\sigma + \mathrm{e}\mu S_{ph}. \tag{9}$$

Many atmospheric electricity models [17,25,26] implicitly assume that $(\nu_i - \nu_a)\sigma$ dominates over $\mu\nabla \cdot \mathbf{j}$ and $\mathrm{e}\mu S_{ph}$, thus reducing (8) and (9) to

$$\partial_t \rho_i = (\nu_i - \nu_a)\sigma/\mu, \tag{10}$$

$$\partial_t \sigma = (\nu_i - \nu_a)\sigma. \tag{11}$$

We remark that

1. Models in [17,25,26] include also the ionic conductivity $\sigma_i = \mathrm{e}\mu_+ n_+ + \mathrm{e}\mu_- n_-$, which we have neglected (see main text).

2. Equation (10) is decoupled from (7) and (11) and therefore it can be and is usually left out from atmospheric models.

The simplifications leading to (10) and (11) amount to neglecting photo-ionization and assuming that electron transport does not significantly alter the ambient conductivity, thus obtaining a weakly non-linear system of equations. This assumption is valid for smooth density profiles but breaks down when strong gradients are present. It must be stressed that streamers are a strongly non-linear process and the terms neglected in (11) play an essential role in their inception and propagation.

DOI: 10.1038/NGEO662
nature geoscience

OPTICAL EMISSIONS

To compare the outcome of our simulation with the optical observations of sprites, we implemented the model of sprite emission described by Liu and Pasko[12]. The model includes a local-field-dependent excitation by electron impact of the $B^3\Pi_g$ and $C^3\Pi_u$ states of N_2 and the $B^2\Sigma_u^+$ state of N_2^+. If they are not quenched, these states relax to their ground state by emitting photons in the first and second positive bands of N_2 and the first negative band of N_2^+. We used the excitation, quenching and emission rates detailed in Table 1 of [12], corrected by altitude-dependent number densities of air molecules. In this paper we report only the emissions from the first positive band of N_2, which is responsible for most of the intensity recorded in ground based observations.

The intensities recorded in direct observations of sprites correspond to the emissions from an integrated line-of-sight perpendicular to the plane of the camera. The finite opening time of the camera — or, in the case of [9], the phosphor persistence of the intensifier — is simulated in our case by averaging over a time of 0.25 ms.

The result appears in Figure 2. The emissions from the emerging streamer head are approximately $1.2 \cdot 10^9$ Rayleigh (1 Rayleigh, abbreviated 1 R, is 10^{10} photons per second per square meter), in agreement with the estimations of [11].

In Figure 6c we show the optical emissions around the emerging streamer at time 4.42 ms. From these optical emissions we can estimate a visible diameter of the streamer of approximately 600 m.

SIMULATED ELECTRIC FIELDS

Our simulations are based on a classical gas discharge model, and therefore, of course, support the classical breakdown model for sprites: to initiate a sprite, the cloud charge must generate local electric field strengths E above the breakdown threshold E_k. The occurrence of this necessary criterion is investigated in [25,26], but not whether subsequently a sprite is actually formed. The evolution of the reduced electric fields E/E_k for the time steps of Figures 1 and 2 is represented in Figure 4. We recall that E_k strongly depends on altitude and that in regions with $E/E_k > 1$, the ionization grows while elsewhere it decreases.

A zoom into the emerging sprite streamer at time $t = 4.42$ ms is shown in Fig. 6. The figure shows a typical positive streamer that propagates in the high-field region due to photo-ionization.

DOI: 10.1038/NGEO662

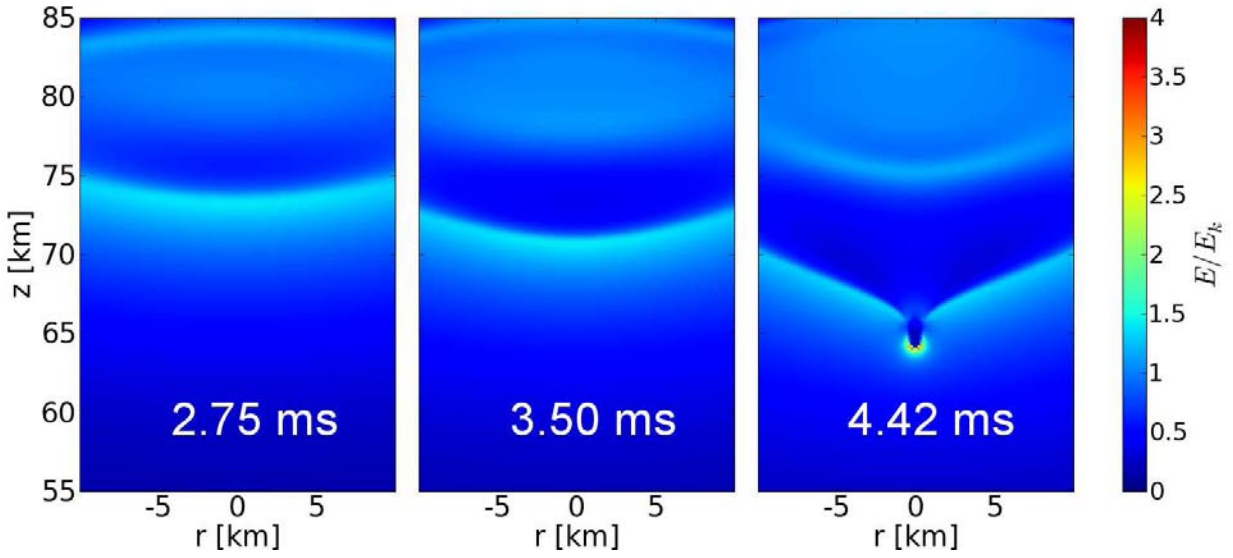

FIG. 5: Reduced electric fields corresponding to the simulation of Figures 1 and 2. Shown is here the reduced electric field strength E/E_k where E_k depends on density and therefore on altitude. The electron density grows due to ionization reactions where $E/E_k > 1$.

The streamer emerges from the tip of the screening-ionization wave where the electric field is focused due to the curvature of the front. The field enhancement in the streamer head is about 4 times E_k.

At time $t = 2.46$ ms of Fig. 2 in Ref. [9], the single initial sprite streamer breaks up into many channels. The same happens in our simulation as well after about 2 km of propagation. However, as we have implemented cylindrical symmetry around the cloud charge axis to reduce computational complexity, the evolution is not physical anymore after branching and therefore not shown.

HORIZONTAL INHOMOGENEITIES

In our reported simulations the initial electron density depends only on the altitude and is thus uniform in the horizontal direction. However, many atmospheric processes such as meteor trails, gravity waves and the previous electrical activity of the thunderstorm may create horizontal inhomogeneities.

Presently our model is limited to cylindrically symmetrical configurations and we could only introduce inhomogeneities with cylindrical symmetry. In particular, we tested the effect of pertur-

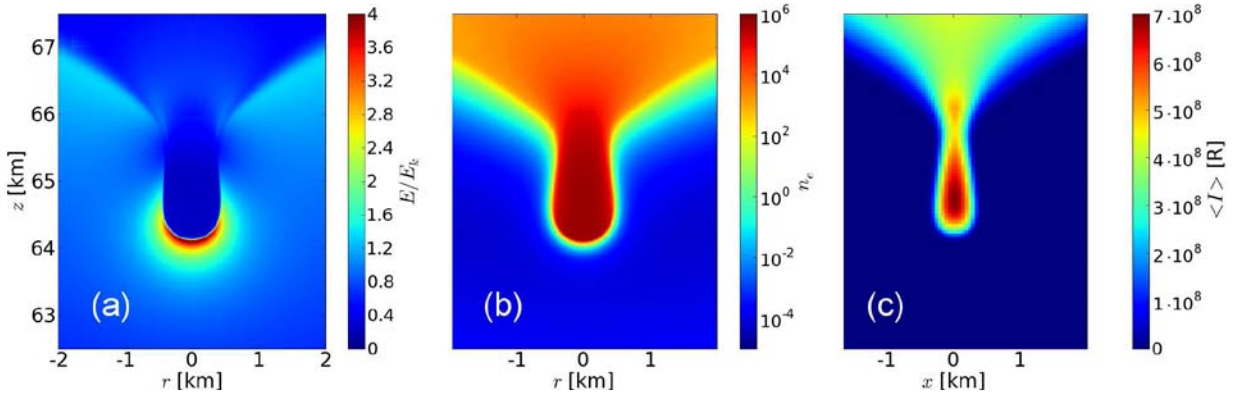

FIG. 6: Zoom into the last time step $t = 4.42$ ms of Figures 1, 2 and 4 showing (a) the reduced field, (b) the electron density and (c) the optical emissions averaged over the previous 0.25 ms.

bations to the initial density of the form

$$n'_e(r,z) = n_e(z)\left(1 + \epsilon e^{-r^2/R^2}\right), \tag{12}$$

where $n_e(z)$ is the unperturbed electron density (plotted in Fig. 4), ϵ measures the amplitude of the perturbation and R determines its width.

When we run a simulation using $\epsilon = 0.2$ (i.e., the maximum increase of electron densities is 20%) and $R = 500$ m, we found that sprites emerge after 3.30 ms at 71 km altitude and for a charge moment change of about 1000 C km. The emerging sprite has an optical diameter of about 250 m and propagates at $\sim 2.5 \cdot 10^7$ m/s. The calculated optical emissions from this sprite are shown in Figure 7: note that in this case the sprite looks dimmer due to the lower charge moment change.

The probable reason is that the horizontal inhomogeneity triggers the instability of the screening-ionization wave much earlier. This effect could explain the observation of sprites produced by flashes with very low charge moment changes that do not generate sprites in a horizontally homogeneous model.

LATERAL EXTENSION

Computer memory limited the spatial extension of the simulation. Adaptive refinement allowed us to use a high resolution only in the interesting areas but we used relatively high resolutions in the complete leading edge of the wide ionization front to avoid matching problems between different levels of resolution. The result is that we run out of memory when we tried to simulate domains

DOI: 10.1038/NGEO662

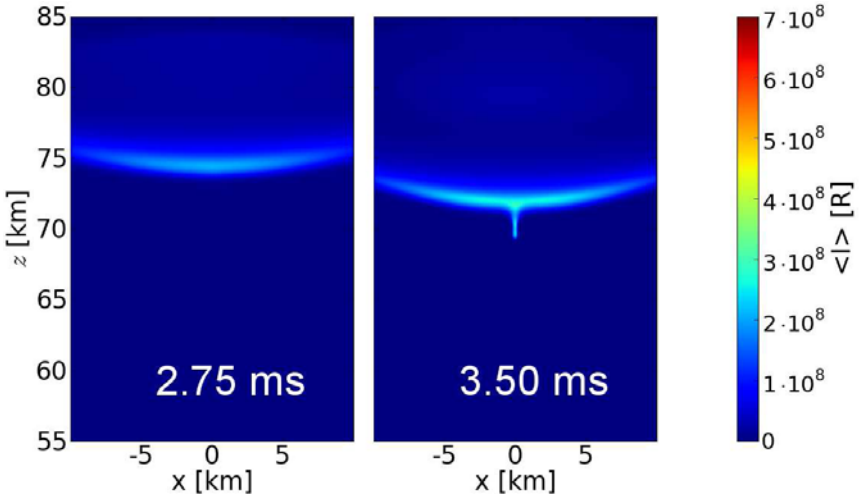

FIG. 7: Optical emissions of a simulation where the initial electron density was perturbed by a horizontal inhomogeneity (see text). We have used the same color scale as in Figure 2 to show that in this case the streamer looks much dimmer. Note that in this case the sprite emerges above 70 km altitude, in closer agreement with observations.

wider than about 20 km. However, since high resolution is not needed in the initial halo stage, we can compare our results with those obtained in a much wider domain, but with a low resolution ($\Delta r = \Delta z = 150$ m) everywhere. The results are shown in Fig. 8.

DOI: 10.1038/NGEO662
nature geoscience

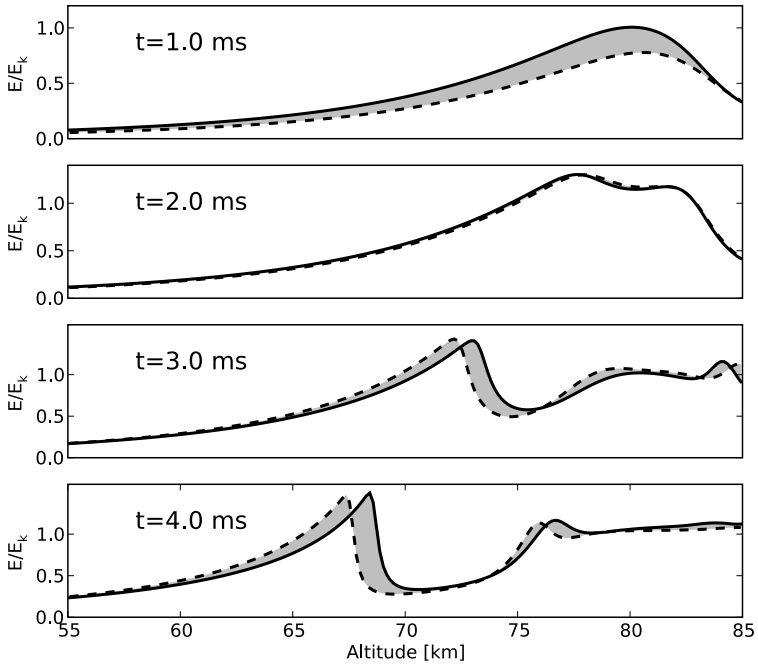

FIG. 8: Comparison between the reduced electric field from a simulation with a maximum radial extension of 20 km (as used in the main text; solid line) and one with 80 km (dashed line). Although there is some difference, the qualitative behavior of both simulations is remarkably close. In particular, the maximal field enhancement is similar.